Monazomycin-induced Single Channels

II. Origin of the Voltage Dependence
of the Macroscopic Conductance

ROBERT U. MULLER and OLAF S. ANDERSEN

From the Department of Physiology, Downstate Medical Center, State University of New York, Brooklyn, New York 11203; and the Department of Physiology and Biophysics, Cornell University Medical College, New York 10021

ABSTRACT   The voltage dependence of the conductance induced in thin lipid membranes by monazomycin is shown here to be caused by voltage-dependent variations in the frequency of channel openings. We also experimentally demonstrate certain interesting properties of the channel activity that are predicted by a chemical kinetic model (Muller and Peskin, 1981), which successfully describes the macroscopic conductance. We conclude that two parallel mechanisms—one autocatalytic, the other simple mass action—exist that allow monazomycin to enter (or leave) the membrane so that the monazomycin molecules can be in a position to form channels.

INTRODUCTION

This is the second of two articles that describe the elementary events that underlie monazomycin-induced conductance (G) changes in planar lipid bilayers. In the preceding article (Andersen and Muller, 1982), we showed that the only characteristic of monazomycin channels that is not nearly invariant to changes in membrane potential (V) is the frequency of occurrence of the channels (f). The purpose of this paper is to show that variations in channel frequency are indeed the basis for the voltage dependence of the monazomycin conductance. It may at first seem incongruous that eliminating all other possible mechanisms was not sufficient to prove that changes of f are the origin of the voltage dependence of G, but in fact the connection was quite difficult to achieve.

The experimental protocol required to explain the voltage dependence of the macroscopic conductance (G) is, in principle, straightforward. The membrane potential should be clamped for a sufficiently long time to allow f to reach its stationary level, f_∞. If this is repeated at various values of V, we can find the function $f_\infty(V)$. Because G is proportional to f (Andersen and Muller,

1982), and because the steady state conductance (G_∞) varies exponentially with V (Muller and Finkelstein, 1972), we expect to find that

$$f_\infty(V) = f_* e^{nqV/kT} \tag{1}$$

where f_* is the (extrapolated) value of f_∞ at $V = 0$, n is an empirical parameter determined from the slope of the G_∞ vs. V line $(n \approx 5)$, q is the electronic charge, k is Boltzmann's constant, and T is the temperature in Kelvin.

We have done the proposed experiment many times and have found that Eq. 1 fails miserably in a substantial fraction of the cases, albeit a fraction that gradually decreased as we gained more experience with the system. (Bamberg and Janko [1976] reported a complete inability to see voltage-dependent behavior at the unitary level.) On some occasions f_∞ was very weakly dependent on V, to the extent that f_∞ would remain fixed after small voltage steps ($|\Delta V| \leq 10$ mV). In other cases, f_∞ would actually decrease when V was raised. In still other cases, f would not go to a steady level at fixed V but would rather fluctuate widely and would often, for no apparent reason, drop to zero and stay there, even when V was increased by 20 mV or more, to levels that had previously supported a respectable channel activity. (Disappearance of channels was not correlated with changes in the visual image of the membrane nor with changes in the background current noise.)

Another very interesting peculiarity was the difficulty we encountered in initiating channel activity in virgin films (or in films in which f goes to zero). We rarely found it possible to obtain single-channel activity merely by clamping to a voltage that experience had taught us was associated with (at the given monazomycin concentration) an analyzable level of f (i.e., the probability of having two or more simultaneously open channels is low). Rather, we generally had to apply potentials much greater than those in the working voltage range (say, 400 instead of 200 mV) to see any activity.

Despite these vagaries, certain features of the voltage dependence of f did gibe with our expectations from experiments on the microscopic (i.e., many channels in a large membrane) conductance. Large changes of $V(|\Delta V| \leq 25$ mV $\approx kT/g)(f \neq 0)$ lead to qualitatively appropriate changes in f (f tends to increase with $+V$ and decrease with $-V$, as does G). Furthermore, we could (almost) always cause the channel activity to cease immediately by applying large negative potentials. Again, the dependence of f on the monazomycin concentration ([Mon]) was grossly predictable; a given value of f_∞ would, on the average, be seen with smaller positive potentials if [Mon] was higher. These observations, together with the cases where Eq. 1 was obeyed, convinced us that the channels are indeed the events that sum to form the macroscopic conductance.

How then is it possible for the voltage dependence of f to be seemingly inconsistent when the voltage dependence of G_∞ is so easy to characterize?[1]

---

[1] We hope it is clear that the complex behavior of f is not caused merely by the fact that we are dealing with fluctuations of the number of open channels. f_∞ is of course a time average; we are concerned with why the time average (f_∞) is sometimes drastically different than the space average (G_∞).

We will demonstrate, in a qualitative fashion, that the resolution of the paradox lies in understanding the nature of the process whereby monazomycin enters and leaves the membrane. The autocatalytic insertion (and removal) of monazomycin, which forms the basis for explaining the kinetics of the macroscopic conductance (Muller et al., 1981; Muller and Peskin, 1981), is formally incompatible with the possibility of ever seeing channel activity in a virgin film. There must exist a second, nonautocatalytic process that allows monazomycin to enter a film that does not yet contain any monazomycin. It is the interplay of these two processes and the existence of detectable correlation times of 10^3–10^4 s (Muller and Peskin, 1981) that leads to the untoward behavior of f. (Some of this material has appeared in abstract form [Muller and Andersen, 1975, 1980]).

MATERIALS AND METHODS

The experimental procedures are similar to those described in the preceding paper. The only difference is that in some of the experiments presented here we took advantage of the possibility of simultaneously voltage clamping a large film (area ≈ 1.3 mm^2) and a small membrane (area $\approx 10^{-4}$ mm^2) that was adherent to a micropipette.

Fig. 1 is a schematic diagram of the experimental set-up. The two films could be clamped to the same potential by applying a voltage between a single electrode in the *cis* chamber and two separate electrodes held at virtual ground by current-to-voltage converters. (As stated in the preceding paper, *cis* refers to the solution to which monazomycin is added. Conductance increases are associated with making the *cis* solution positive with respect to the virtual grounds.) One virtual ground electrode was in the bulk solution of the *trans* chamber, whereas the other was in the lumen of the micropipette that supported the small film.

We found this arrangement to be satisfactory if great care was taken to set the outputs of the two current-to-voltage converters to zero when $V = 0$, in the absence of membranes. If this was not done, merely moving the pipette tip back into the *cis* chamber, and thereby destroying the small film, would cause changes in the potential difference across the large membrane (as measured by changes in the monazomycin-induced conductance). Such voltage shifts arise if significant current must flow through the large membrane just to keep the potential of the pipette electrode at virtual ground. It was crucial to avoid such shifts, because our experimental protocols required us to keep the state of the large film constant as we captured several small films, one after the other.

THEORY

We present here a simplified version of a kinetic model that has been shown to account for many of the properties of the macroscopic monazomycin conductance (Muller et al., 1981; Muller and Peskin, 1981). We intend to demonstrate that the very complicated relationship between channel frequency and membrane potential briefly mentioned in the introduction is (at least in a qualitative way) predicted by the model. In fact, the results we will discuss below lend very strong support to the essence of the model, namely the assumption that entry and exit of monazomycin from the membrane is autocatalytic in nature; the experimental outcomes we report seem to us incomprehensible without the autocatalytic process.

The forms of macroscopic monazomycin conductance changes are accurately fitted by solutions of Eq. 2:

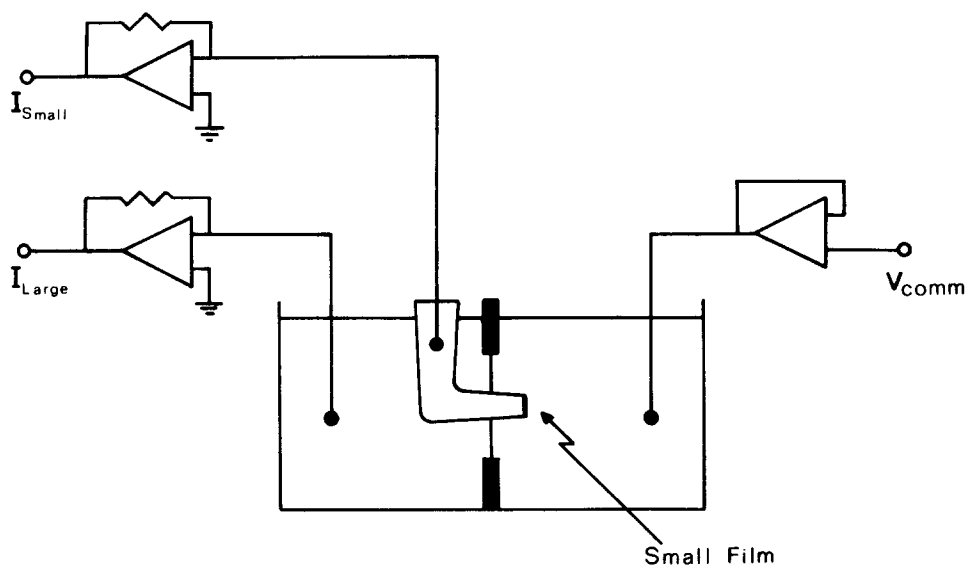$$\frac{dG}{dt} = AG\left[1 - \left(\frac{G}{G_\infty}\right)^B\right].$$

(2)

FIGURE 1. Schematic diagram of the experimental set-up used to simultaneously clamp a large and a small membrane to the same potential and to measure the current flowing through each independently. Monazomycin is added to the right-hand compartment (which is designated "cis"); the solution on the trans side of both membranes is held at virtual ground by independent current-to-voltage converters. This arrangement allows us to monitor the current through both membranes at the same time, a capability which is used in the experiments of Figs. 2–6 and 8. In each of these cases, the cis and trans solutions were 1.0 M NaCl rather than the 0.1 M NaCl used in all other experiments. The higher salt concentration ensured essentially instantaneous sealing of the small film onto the pipette (see Materials and Methods of Andersen and Muller, 1982). Also note that in each case where the capture of a small membrane is shown there are two manipulations of the pipette. The first is withdrawal of the pipette into the trans solution followed by insertion of the tip into the torus of the large film. This procedure effectively "washes" the pipette clean of the first small film. The second manipulation is removing the pipette from the torus and then pushing it through the thin phase of the large film to get the new small film.

The parameter B ($B = 0.7$) is a constant for the monazomycin-PGC (PGC stands for membranes prepared from a 1%/1% [wt/wt/vol] solution of phosphatidylglycerol plus cholesterol in n-decane solution) membrane system over a rather wide range of [Mon] and V. The rate constant, A, and G_∞ are functions of [Mon] and V:

$$A = A_* \left(\frac{[\text{Mon}]}{[\text{Mon}]_*}\right)^3 e^{3qV/kT}; \tag{3}$$

$$G_\infty = G_* \left(\frac{[\text{Mon}]}{[\text{Mon}]_*}\right) e^{6qV/kT}. \tag{4}$$

A_* and G_* are, respectively, A and G_∞ at $V = 0$ and at a reference monazomycin concentration ($[\text{Mon}]_*$). The simplifications of the model are: (a) assigning integer values of the exponents in Eqs. 3 and 4; (b) letting the concentration-dependence exponents equal the voltage-dependence exponents; (c) setting the exponents for A to exactly one-half the exponents for G_∞. (Accurate values for the 4 exponents are given in Muller et al., 1981.)

Eqs. 2–4 can be derived from a chemical kinetic scheme that contains the following steps:

aqueous trimerization (equilibrium):

$$3M \xrightarrow{\ K_0\ } M_3; \tag{5}$$

insertion of monazomycin into the membrane (rate limiting):

$$M_3 + \widetilde{M}_3 \underset{k_-(V)}{\overset{k_1(V)}{\rightleftharpoons}} 2\widetilde{M}_3; \tag{6}$$
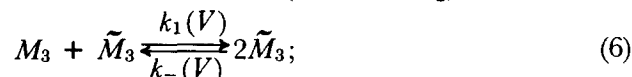
channel formation (equilibrium):

$$2\widetilde{M}_3 \xrightarrow{\ K_2\ } \widetilde{M}_6. \tag{7}$$

M, M_3, $\widetilde{M}_3$, and $\widetilde{M}_6$ are various states of monazomycin molecules. M is aqueous monomer. M_3 is aqueous trimer and is the species that can shuttle into and out of the membrane. The concentration of both aqueous species is constant, because not enough monazomycin can enter the film to reduce the amount added to the *cis* solution. Nonconducting, membrane-bound trimers are designated $\widetilde{M}_3$. Two $\widetilde{M}_3$'s must aggregate to form one $\widetilde{M}_6$, the conducting channel.

Reaction 6 is the crucial part of the channel-formation process. In the first place, it is the source of the voltage dependence. Reaction 6 describes a partitioning of trimer between the *cis* aqueous solution and the membrane. The magnitude of the partition coefficient is voltage dependent because the positive charge of the monazomycin (monazomycin is a univalent cation at neutral pH) must move through the membrane field from the *cis* to the *trans* interface.[2] The importance of the insertion step is further emphasized by

[2] Our physical picture of the state of membrane-bound monazomycin (Heyer et al., 1976; Muller and Peskin, 1981), which is fully corroborated by the structure of monazomycin (Nakayama et al., 1981), can be summarized as follows: (a) a single monazomycin molecule is long enough to span the membrane; its length is ~40 Å, from measuring a CPK model. (b) The spanned molecules must form aggregates that are cylindrical micelles arranged so that the outer, lipophilic surface of the monazomycin molecules is exposed to hydrocarbon of the membrane, whereas the inner, hydrophilic surfaces are mutually shielded from the membrane interior. We presume that spanned monomers are very unlikely because of the large number of hydroxyl groups that would be in direct contact with the membrane hydrocarbon.

asserting that the equilibrium of reaction 7 lies far towards the $\tilde{M}_3$ form (Muller and Peskin, 1981). Because $\tilde{M}_6$ constitutes a negligible fraction of the total membrane-bound monazomycin, from a mechanistic viewpoint we may consider the channels as no more than a convenient way of monitoring the surface concentration $[\tilde{M}_3]$.

The most interesting feature of the kinetic scheme is the appearance of an "extra" $\tilde{M}_3$ on both sides of reaction 6. This cannot affect the position of the equilibrium, but it is crucial for the kinetic behavior. The extra $\tilde{M}_3$ expresses the autocatalytic nature of reaction 6: because M_3 is fixed, the (surface) concentration of $\tilde{M}_3$ determines [along with the rate constants $k_1(V)$ and $k_{-1}(V)$] the instantaneous reaction rate.

The autocatalytic property of reaction 6 has two very important consequences. First, it determines the observed shapes of conductance changes after voltage steps (Muller et al., 1981). Second, it makes the approach to equilibrium upon reducing the voltage extraordinarily slow at low $[\tilde{M}_3]$ (i.e., low conductance). This is because two M_3's must meet for one of them to leave the film; such events will become extremely rare when $[\tilde{M}_3]$ is low. (There is no discrepancy between a very slow desorption rate and a very low but steadily declining channel frequency, even though both channel formation and desorption depend on encounters of $\tilde{M}_3$, if the probability of channel formation [reaction 7] is more likely than the probability of desorption.)

In a general way, the complex f vs. V behavior of monazomycin-treated films is now comprehensible; the very long relaxation times made possible by the autocatalytic insertion step in turn make the instantaneous value of f a function of the history of stimulation (or equivalently, a function of the experimental protocol). In the Results (*Origin of the Voltage Dependence*), we will show that the steepness of the log f_∞-V line can be varied at will simply by selecting the sequence of voltage steps used to measure f_∞. First, however, we must consider two deficiencies of the model as so far presented and the implications of a more realistic treatment.

One difficulty with the model expressed in Eqs. 2–4 lies in its disregard of molecules as countable particles; all of the concentrations are expressed as continuous quantities. Although this is perfectly acceptable at high G_∞ (and therefore high $[\tilde{M}_3]$), at low G_∞ the average distance between $\tilde{M}_3$ aggregates must increase to the point that exit of monazomycin will be limited by lateral diffusion times rather than by the rate at which reaction 6 proceeds. If a positive voltage step is imposed on a membrane in which the $\tilde{M}_3$ complexes are far apart, the autocatalytic entry of M_3 will initially go on normally at the loci of the remaining $\tilde{M}_3$ and not at all in between them. A molecular interpretation of the autocatalytic hypothesis thus requires that the film be pictured as inhomogeneous when $[\tilde{M}_3]$ is very low (i.e., the space average loses significance). As we will demonstrate below, this inhomogeneity is an observable property of the system.

The second problem with the model is simply that it cannot be complete as stated. Although it describes the behavior of active films, it precludes transitions in either direction from inactive to active. This is evident from reaction 6, which will not proceed if $[\tilde{M}_3] = 0$. Moreover, if $[\tilde{M}_3] \neq 0$, there is no basis

on which the $[\tilde{M}_3] = 0$ state can be reached. (Alternatively, we can say that Eq. 2 admits of the trivial solution: $G = 0$ and $\dfrac{dG}{dt} = 0$. No mechanism exists in reactions 5–7 that allows for transitions between this solution and solutions such that $G > 0$. This is a general problem in systems that exhibit autocatalysis; an ability to describe temporal variations in population size does not speak to the question of how the first members of the population can appear on the scene.)

From the fact that it is possible to switch between the active and inactive states, we are led to conclude that a nonautocatalyzed reaction pathway must exist in parallel with reaction 6. The simplest such reaction is:

$$M_x \underset{k_{-3}(V)}{\overset{k_3(V)}{\rightleftharpoons}} \tilde{M}_x, \tag{8}$$

where x is the molecularity of the oligomer that enters and leaves the film. If $x = 3$, the equilibrium constants for reactions 6 and 8 are the same. We can also infer that the rate constants for reaction 8 are very small compared with those for reaction 6 from the observation that the behavior of the membrane is generally dominated by reaction 6 (even at very low monazomycin-induced conductance). The existence of a nonautocatalytic insertion process is also a demonstrable feature of this system.

RESULTS

Experiments with Large and Small Films

DEPENDENCE OF THE INITIATION OF CHANNEL ACTIVITY ON MEMBRANE AREA   In Fig. 2, we show the results of simultaneously stepping the potential across a large ($A_l = 1.3$ mm^2) and a small ($A_s = 10^{-4}$ mm^2) membrane from -160 to $+160$ mV. The protocol was to first clamp the large membrane to -160 mV, to ensure it was put into the unmodified state. The micropipette was then pushed into the large film, thereby capturing a small film; in the 1.0 M NaCl used in these experiments, the seal took place almost instantaneously (see Materials and Methods of the preceding paper). The sign of the potential was then reversed with the result that G for the large film increased in the characteristic (for monazomycin) S-shaped fashion to a steady state. Meanwhile, the small film remained completely silent.

We interpret this strange result in terms of the very disparate membrane areas and the necessarily small value of the mass-action rate constant for insertion $[k_3(V)]$.[3] If $k_3(V)$ is the same for both films, the absolute rate at which reaction 8 proceeds is proportional to membrane area. It therefore must be easier to drive the larger film from the inactive to the active state. In principle, it requires the insertion of only one X-mer via reaction 8 for the

---

[3] We have arranged the ionic environment and the electrical situation to be identical for the two membranes. Moreover, so far as we have investigated, the small film has the same properties as the large; for instance, gramicidin A channels have the same conductance independent of film area (Andersen, unpublished observations). We conclude that the present difference in behavior of the large and small films is only a function of area.

conductance to go relatively rapidly to its equilibrium value. Once at least one seed has entered, the whole film can become modified due to lateral diffusion coupled with additional entry via reaction 6. It is therefore possible for the large film to arrive at a high conductance while the small film remains quiescent, because the probability of the single necessary insertion event is higher for the large film by the ratio of A_l/A_s ($\sim 10^4$).

We repeated the sequence shown in Fig. 2 six times in one experiment. In five of the cases, no activity was seen in the small film, even though the potential was held at +160 for $\sim$5 min each time. The behavior for the last 40 s of the final case is presented in Fig. 3, and is particularly instructive. Here, the small film stayed inactive for most of the time it took the large one to
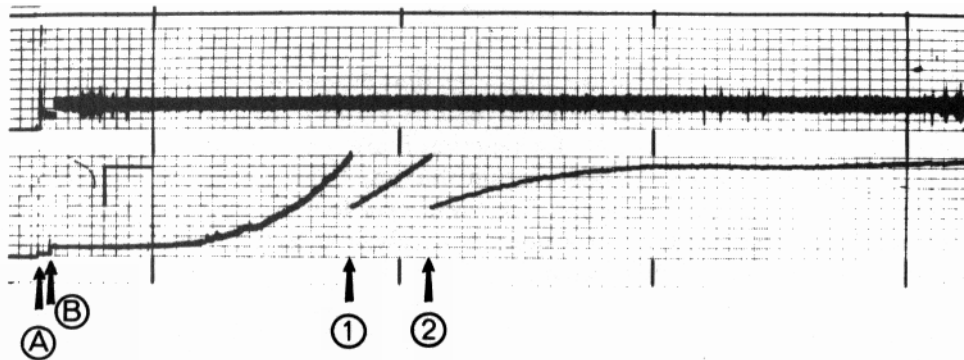

FIGURE 2.   Behavior of a small film captured from an inactive large film. The upper trace shows the current through the small film, low-pass-filtered at 100 Hz. The bottom trace shows the large film current. The small film is in place before the beginning of the record; it was taken with the large film held at -160 mV. At arrows A and B, V was briefly switched to 0 and then to +160 mV. The large membrane shows the typical (for the monazomycin conductance) S-shaped conductance increase to a steady state. Meanwhile, the small membrane was completely quiescent. (The brief pen deflections in the upper trace are mechanically induced artifacts; these are characteristically symmetrical around the noise envelope.) Horizontal calibration mark = 20 s. Vertical calibration mark, upper trace = 10^{-12} A. Lower trace: left side to arrow 1 = 10^{-9} A; arrow 1 to arrow 2 = 2×10^{-9} A; arrow 2 to right side = 4×10^{-9} A.

reach G_∞. Note, however, that some 230 s after the switch to +160 mV, channel activity abruptly began. This fortuitous entry of an M_3 into the membrane at the relatively low value of +160 mV shows that the probability of a seed getting in via reaction 8 is indeed low, but not zero. Presumably, had we waited long enough, all trials using this protocol would have resulted in small-film channel activity.

The astute reader will by now have wondered what happens if the small film is captured while the large film is clamped to +160 mV and is at G_∞. The result of this manipulation is shown in Fig. 4. As expected, the small film showed immediate channel activity. We also repeated this sequence six times (actually alternating with the first sequence) and found the same outcome

each time. Thus, if the piece of the large membrane captured by the pipette already contains monazomycin, reaction 8 becomes superfluous. As we shall show below, capturing a small film from an active large one is the protocol of choice if one is interested in studying channel statistics in the steady state, because it eliminates many of the vagaries associated with the nonautocatalytic reaction.
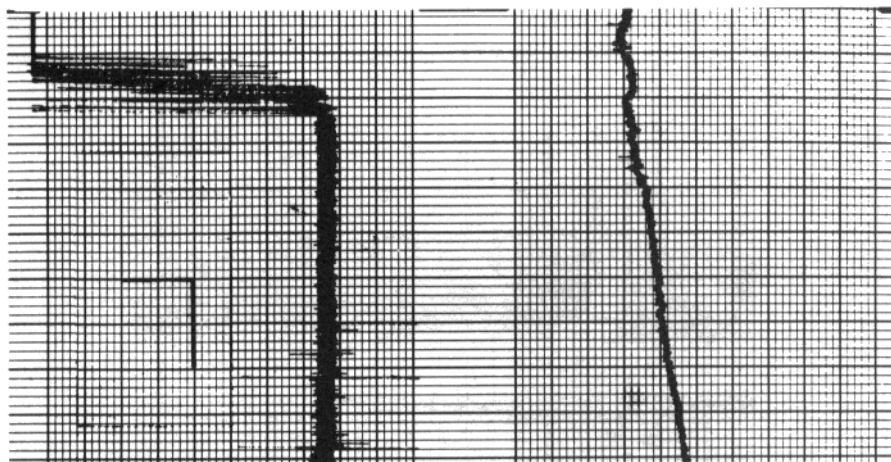

FIGURE 3. "Spontaneous" beginning of channel activity in a small film captured from an inactive large film. This is the end of a record obtained using exactly the same protocol as in Fig. 2. The switch from -160 to $+160$ mV was made 200 s before the record shown here, during which time the small film was completely inactive while the conductance of the large film was increasing. The small film (upper trace) remained inactive for an additional 28 s and then abruptly showed channel jumps. The "hash" near the right side of the record is the channel activity. It is visible for only 7 s before the pen reached its limit. Here, as in Figs. 4–6 and 8, individual channels were easily visualized on an oscilloscope whose beam was driven in parallel with the small membrane pen-writer recording. Horizontal calibration mark = 10 s. Vertical calibration mark, upper trace = 5×10^{-13} A; lower trace = 5×10^{-9} A.

SPATIAL INHOMOGENEITY OF MONAZOMYCIN-MODIFIED MEMBRANES DURING CONDUCTANCE INCREASES Fig. 5 shows an experiment in which three small films were taken during the conductance increase of a large film after a voltage step from -160 to $+160$ mV. This procedure was possible only because of the slow kinetics of this system. The first two small films were inactive, whereas the third showed channel activity as soon as it was captured.

We have already shown that the noncatalyzed entry of a single M_3 seed is sufficient to start channel activity. Also, the diameter of the micropipette is much greater than the average distance between $\tilde{M}_3$ aggregates at the level of G that had been reached when the second film was taken. (Assume that $\tilde{M}_3$ is homogeneously distributed in the large membrane. From Eq. 10 of Muller and Peskin [1981], with $B = 5$ and $K_2 = 7.5$ [a worst-case choice], $[\tilde{M}_3]$ can be

estimated as 7.7×10^{-14} M·dm^{-2} at $G = 10^{-9}$ Ω^{-1} in a 1-mm^2 membrane. If $A_s = 10^{-4}$ mm^2 $= 10^{-8}$ dm^2, there should be about 500 molecules of M_3 caught in the small film.) We must therefore conclude that the large membrane was not uniformly modified during the conductance increase of Fig. 5. Rather, there are most likely hot spots that are centered on the initial $\tilde{M}_3$ seeds. Presumably, as equilibrium is reached, these hot spots grow in a radially symmetrical fashion and ultimately coalesce, at which time the membrane is spatially uniform with respect to monazomycin concentration.

A DIRECT DEMONSTRATION OF SPATIAL INHOMOGENEITY   During an experiment in which we were monitoring G increases of a large film in response to
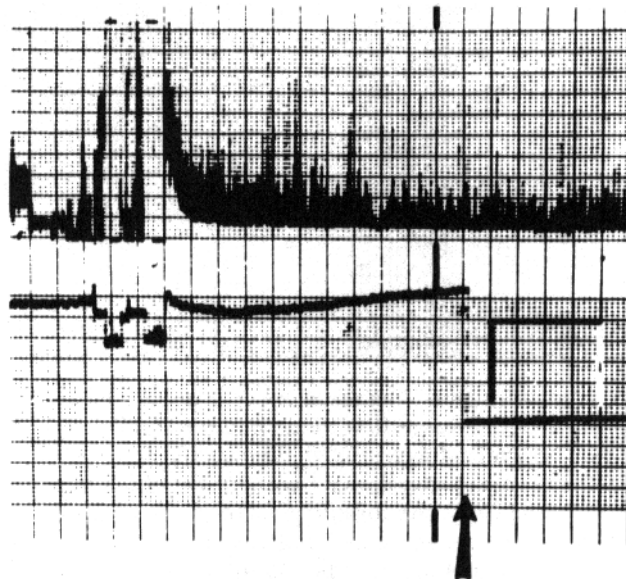

FIGURE 4.   Behavior of a small membrane taken from an active large membrane. The lower trace shows that the current through the large membrane is essentially constant (at $V = +160$ mV) as the small pipette is withdrawn into the *trans* chamber and then reinserted into the large membrane. Note that the small film (upper trace) is active as soon as it is captured. The "hash" visible in the pen-writer trace could be resolved as channel jumps on an oscilloscope. Horizontal calibration mark = 10 s. Vertical calibration mark, upper trace = 2 $\times 10^{-12}$ A; lower trace, left side to arrow = 2×10^{-9} A; arrow to end = 5×10^{-9} A.

positive voltage steps, we saw a case in which G appeared to be reaching an anomalously low level of G_∞. We hypothesized that this might mean that the membrane was only partially modified and proceeded to sample from different places with the micropipette. It proved possible to reliably get active small membranes from one region and silent small membranes from the rest of the membrane. Examples of the responses of small membranes and a map of the large membrane are shown in Fig. 6.

SUMMARY OF TWO-MEMBRANE RESULTS   We feel that the experiments using large and small membranes strongly corroborate the picture of the monazo-

mycin-induced conductance provided by reactions 5–8. The existence of parallel autocatalytic and nonautocatalytic insertion pathways (reactions 6 and 8, respectively) with very different rate constants also allows us to account qualitatively for two puzzling phenomena mentioned in the introduction. The first is the need to use very intense stimulation to turn on a silent small film. Because the actual rate for reaction 8 is proportional to membrane area, $k_3(V)$ must be set to a very high level to yield a relatively short waiting time for a nonautocatalytic entry of an M_3 into a small film.[4] As a corollary, the high
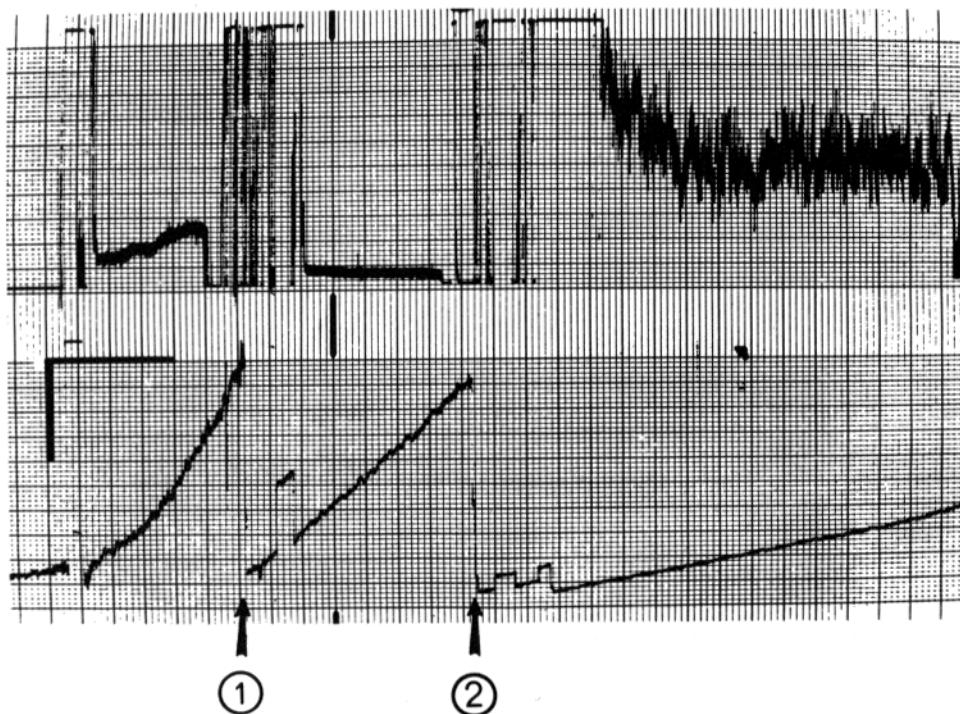

FIGURE 5. Inhomogeneity of membrane modification during a conductance increase in a large film; the conductance had not yet reached a steady state at the end of the illustrated record. At $t = 0$, a step from 0 to +200 mV was made; the first 68 s at 200 mV are now shown. At $t = 82$, 115, and 155 s, three small membranes were taken. At the stated times, the approximate conductance of the large film was 3×10^{-10}, 7×10^{-9}, and 2×10^{-8} Ω^{-1}. The first two small films were inactive, whereas the third showed channel activity as soon as it was taken. Horizontal calibration mark $= 20$ s. Vertical calibration mark, upper trace $= 2 \times 10^{-12}$ A; lower trace, from left side to arrow $1 = 4 \times 10^{-10}$ A; from arrow 1 to arrow $2 = 2 \times 10^{-9}$ A; from arrow 2 to end of record $= 2 \times 10^{-8}$ A.

[4] Note that doing "waiting-time" experiments provides a means of finding the function $k_3(V)$. All that is required is to clamp a silent film to some value of V and measure the time is takes for channel activity to appear; the reciprocal of the average waiting time is k_3 at the selected value of V. $k_{-3}(V)$ can also be measured with waiting-time experiments.

value that $k_1(V)$ will have at the voltages required to initiate channel activity via reaction 8 makes it clear why V must be reduced to resolve individual conductance events.

The second phenomenon that is now comprehensible is the sudden, "spontaneous" cessation of channel activity that may occur during a long run
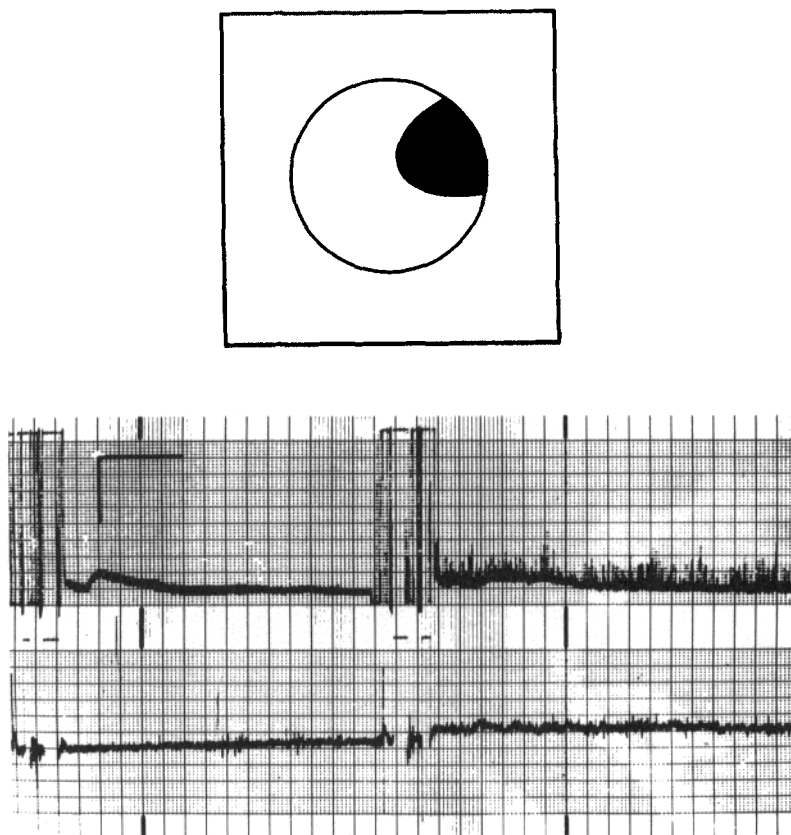

FIGURE 6. Sampling small membranes from an inhomogeneously modified large membrane. The upper trace shows an inactive (left side) and an active (right side) small film which were taken from a large film (lower trace) that had reached an anomalously low conductance ~15 min after a step from $V = 0$ to $V = +135$ mV. The two small films are examples from a sample of 22 small films. The inset shows a "map" of the large film; only active small membrane were acquired from the shaded region ($n = 11$); only inactive small films were taken from the unshaded region ($n = 11$). Horizontal calibration mark = 20 s. Vertical calibration mark, upper trace = 2×10^{-12} A; lower trace = 2×10^{-10} A.

at constant potential. We imagine that at very low channel frequency, it is possible to arrive at a state where a single $\tilde{M}_3$ is left in the film. Under these circumstances, the autocatalytic removal rate constant $k_{-1}(V)$ may be high enough that the most likely fate for a second $\tilde{M}_3$ that enters to form a channel

is to leave the membrane very quickly rather than to diffuse away from the original in the plane of the film. We therefore tentatively suggest that a sudden loss of channel activity (see Fig. 8) must reflect the disappearance of the only $\tilde{M}_3$ in a membrane via the nonautocatalytic pathway (reaction 8).

Origin of the Voltage Dependence of the Macroscopic Conductance

WEAK OR REVERSE VOLTAGE DEPENDENCE   The experiments summarized in Fig. 7 and Table I were designed to show that it is possible to get a weak voltage dependence of channel frequency (Fig. 7) or even to change the apparent sign of the voltage dependence of G (Table I) simply by selecting the
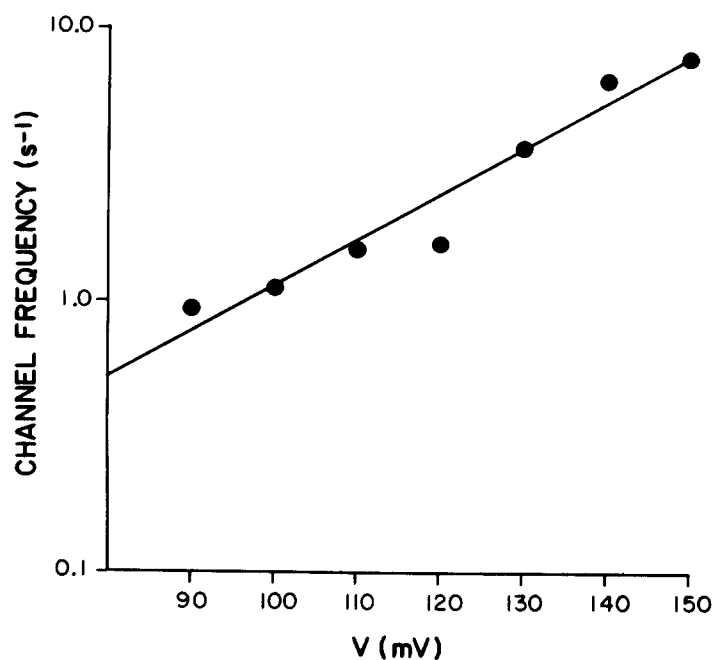

FIGURE 7.   Log f_∞-V plot showing weak voltage dependence of f_∞. In the experiment summarized here, the small film was activated by applying a +200-mV stimulus. The values of f_∞ were obtained starting at +90 mV, in ascending order of applied V. Further description is given in the text.

TABLE I

INVERSE VOLTAGE DEPENDENCE OF G

V	I	G^*
mV	A	Ω^{-1}
110	3.7×10^{-13}	3.4×10^{-12}
125	1.92×10^{-13}	1.5×10^{-12}
140	1.98×10^{-13}	1.4×10^{-12}

* No correction was made for current flow through the unmodified bilayer. The apparent magnitude of the reversal of the voltage dependence of G is therefore less than it actually was.

stimulation protocol. These are really no more than replications of experiments that we did before we realized how crucial the history of stimulation is in this system. It was the existence of results such as these that caused us to be unsure of our ability to account statistically for the voltage dependence of G. Because we can now vary the voltage dependence at will (compare the slopes of the $\log f_\infty$-V lines in Figs. 7 and 9), we feel that the results presented in this section support our theory rather than contradict it.

Essentially the same protocol was used for the experiments of Fig. 7 and Table I. For Fig. 7, an inactive small membrane was taken in the presence of a monazomycin concentration that we knew would support an analyzable level of channel activity at membrane potentials near +100 mV. The small membrane was then clamped at +200 mV until channel activity abruptly began (~5 s). V was then reduced to +90 mV and left there until f had reached an apparent steady state. V was then raised in 10-mV increments (to a final value of +150 mV) and f was allowed to reach an apparent steady state at each level. The $\log f_\infty$-V characteristic is a fairly decent straight line, but the slope is only an e-fold change of f for a 25.7-mV change of V. This is about one-half the slope of the $\log f_\infty$-V line of Fig. 9. For Table I, the same protocol was followed, except that V was reduced to +110 mV after the +200-mV initiating stimulus and then raised twice by 15-mV increments. Here, the average low-pass-filtered current (I_s) actually decreases as V is raised; the sign of the voltage dependence has changed. (Although the apparent steady state level of I_s decreases, we usually find that immediately after V is raised, I_s goes through a transient maximum.)

This weak or reversed voltage dependence is best explained by listing the three outcomes that are possible when V is reduced after channel activity has been initiated with strong stimulation.

(a) The new voltage may be low enough to set $k_{-1}(V)$ and $k_{-3}(V)$ to levels so high that channel activity rapidly ceases. This sort of behavior is routine with $V < -50$ mV.

(b) The new voltage may set the rate constants such that the system goes smoothly to equilibrium, even if the process takes many minutes. Relatively small voltage changes ($|\Delta V| \leq 25$ mV) will allow the system to remain near equilibrium, so that Eq. 1 is obeyed. This kind of behavior is very difficult to achieve with the protocol under consideration. When it is seen, however, the $\log f_\infty$-V line has a slope similar to the one in Fig. 9. (The line in Fig. 9 was obtained with a different protocol.)

(c) The new voltage is between the values that give rise to cases a and b above. The system may then become kinetically "trapped" at an activity level higher than the equilibrium at the applied potential. This is possible because the likelihood of a successful encounter of two $\tilde{M}_3$ (reaction 6) is very small when $[\tilde{M}_3]$ is low. Thus, f will continue to decrease, but at a rate so low that it may appear to be constant for minutes at a time. Under these circumstances, a small positive-going voltage step will produce either a smaller-than-expected increase of f, or, if the system is far enough from equilibrium, will only slow the decline of f, so that the voltage dependence will appear reversed in sign.

We conclude that the kinetic scheme outlined in reactions 5–8 is at least

qualitatively capable of predicting variations in voltage dependence that result from the choice of experimental protocol. We now will show that a protocol that involves taking small films from large ones whose conductance is in the steady state reliably yields $\log f_\infty$-V characteristics that closely conform to expectations derived from $\log G_\infty$-V data.

VOLTAGE DEPENDENCE OF THE MACROSCOPIC CONDUCTANCE RESULTS FROM THE VOLTAGE DEPENDENCE OF CHANNEL FREQUENCY   The pen-writer records of Fig. 8 show the last 12.8 min of an experiment that ran for a total of 22.8 min. At the beginning, we took a small film from a large one that was already active (at $V = 175$ mV). We then applied a series of voltage steps that alternately raised and lowered the conductance of both films. The first step was from 175 to 160 mV. Each positive-going step returned V to 175 mV,[5] and each subsequent negative-going step was 5 mV greater in magnitude than the previous one. Parts A–D of Fig. 8 show, respectively, transitions from 155 to 175 mV, 175 to 150 mV, 150 to 175 mV, and 175 to 145 mV. Changes of the gains of the three traces in each part are marked by arrows in the figure and are numerically specified in the figure legend.

Three major points are illustrated in Fig. 8. First, we note that the ratio $G_{large}/G_{small} \approx 7.5 \times 10^3$ at the ends of Figs. 8A and B and $\sim 12.3 \times 10^3$ at the end of Fig. 8C. This is in reasonable agreement with our estimate of the ratio of the areas, $A_{large}/A_{small} \approx 10^4$ and supports our belief that the large and small films differ only in area. (For five separate measurements of G_{large}/G_{small} in this experiment, the ratio ranged between 6.1×10^3 and 12.3×10^3. The mean value was 8.5×10^3.) Second, along similar lines, Fig. 8 shows that parallel kinetic behavior of large and small films can be observed when the small film is taken from an active large one. This holds true even when the activity of the small film is low enough to permit the resolution of individual channels (Fig. 8B). Finally, Fig. 8D (taken at 145 mV) shows the rather abrupt cessation of channel activity we referred to above. This sort of occurrence is a real feature of the monazomycin system; the loss of activity is not caused by a change of the state of the small film (e.g., a sudden thickening), because no change in the background noise of the "fast" trace of the small membrane current is seen. Subsequently returning V to 175 mV produced the usual S-shaped conductance increase in the large film, but channel activity did not resume in the small film. We have already given our qualitative explanation of this phenomenon in SUMMARY OF TWO MEMBRANE RESULTS.

The most important result of our analysis of the channel basis of the monazomycin-induced conductance is shown in Fig. 9, which is a plot of $\log f_\infty$ vs. V for a small membrane taken from an active large film. The data are from the same experiment presented in Fig. 11B of the preceding paper; a plot of G_∞ vs. V may be obtained by combining information from that figure and the present one.

As is evident from Fig. 9, Eq. 1, which demands that $\log f_\infty$ vs. V be a

---

[5] Actually, because the conductance of the large film was not absolutely stable over the full time course of the experiments, we made minor adjustments of V so that each negative-going step began at the same level of G_∞. In practice, the largest V was 177 mV and the smallest was 174 mV. The ΔV for negative-going steps was always in multiples of 5 mV.
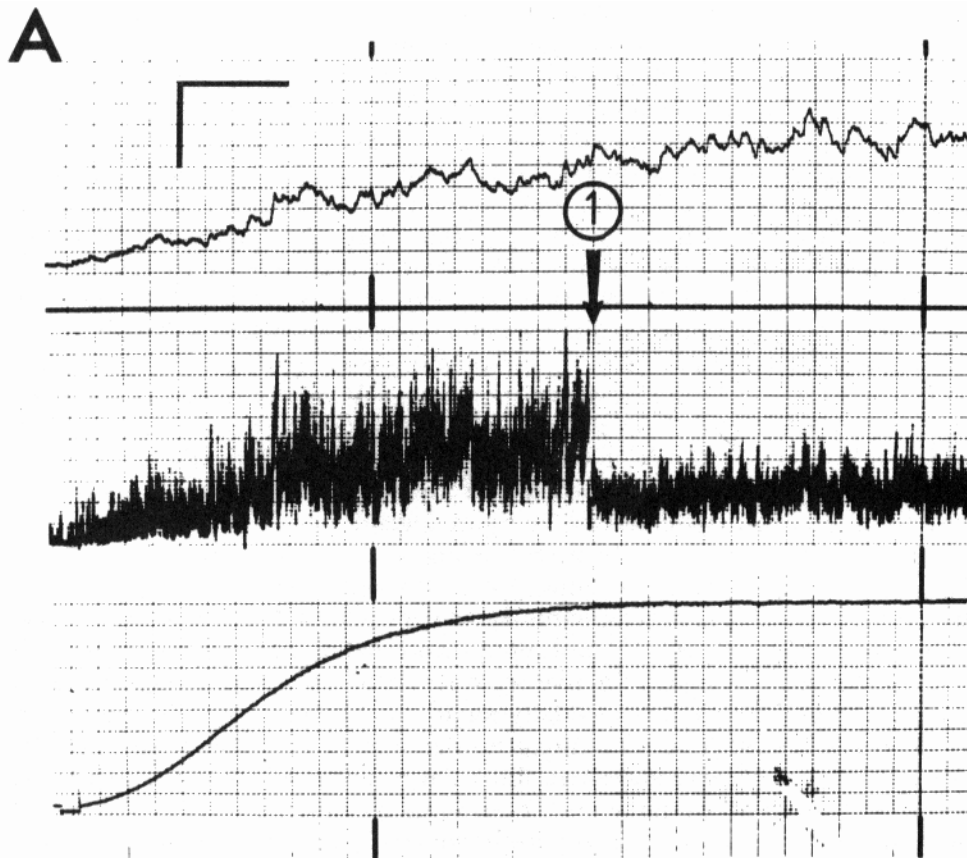
FIGURE 8.   Parallel conductance changes in a large and a small membrane subjected to the same voltage steps. Also shown (in D) is an example of the rather abrupt disappearance of channel activity in a small film. In each part, the upper trace is the low-pass-filtered (1.0 Hz) current through the small film, the middle trace is the "fast" recording (low-pass-filtered at 100 Hz) of the channel activity and the bottom trace is the current through the large film. In all cases, the horizontal calibration mark = 20 s. A. Voltage step from 155 to 175 mV. Vertical calibration mark, upper trace = 4×10^{-12} A; middle trace, from left side to arrow 1 = 4×10^{-12} A; from arrow 1 to end = 10^{-11} A; bottom trace = 2×10^{-8} A. B. Voltage step from 175 to 150 mV. Vertical calibration mark, upper trace = 4×10^{-12} A except between arrows 1 and 2; between arrows 1 and 2 = 4×10^{-13} A; middle trace = 10^{-4} A from the left side to arrow 1. From arrow 1 to arrow 2 = 2×10^{-13} A; from arrow 2 to the end = 4×10^{-12} A; bottom trace, from the left side to arrow 1 = 2×10^{-8} A; from arrow 1 to arrow 2 = 10^{-9} A; from arrow 2 to end = 2×10^{-8} A. C. Voltage step from 150 to 175 mV. Vertical calibration mark, upper trace = 4×10^{-13} A; middle trace = 4×10^{-13} A; bottom trace, left side to arrow 1 = 2×10^{-8} A; arrow 1 to arrow 2 = 4×10^{-8} A; arrow 2 to end = 2×10^{-2} A. D. Voltage step from 175 to 145 mV. Vertical calibration mark, upper trace, from the left side to arrow 1 = 4×10^{-12} A; from arrow 1 to the end = 2×10^{-13} A; middle trace, from the left side to arrow 1 = 4×10^{-12} A; from arrow 1 to the end = 10^{-12} A; bottom trace, from left side to arrow 1 = 2×10^{-8} A; from arrow 1 to the end = 4×10^{-10} A.

B

C
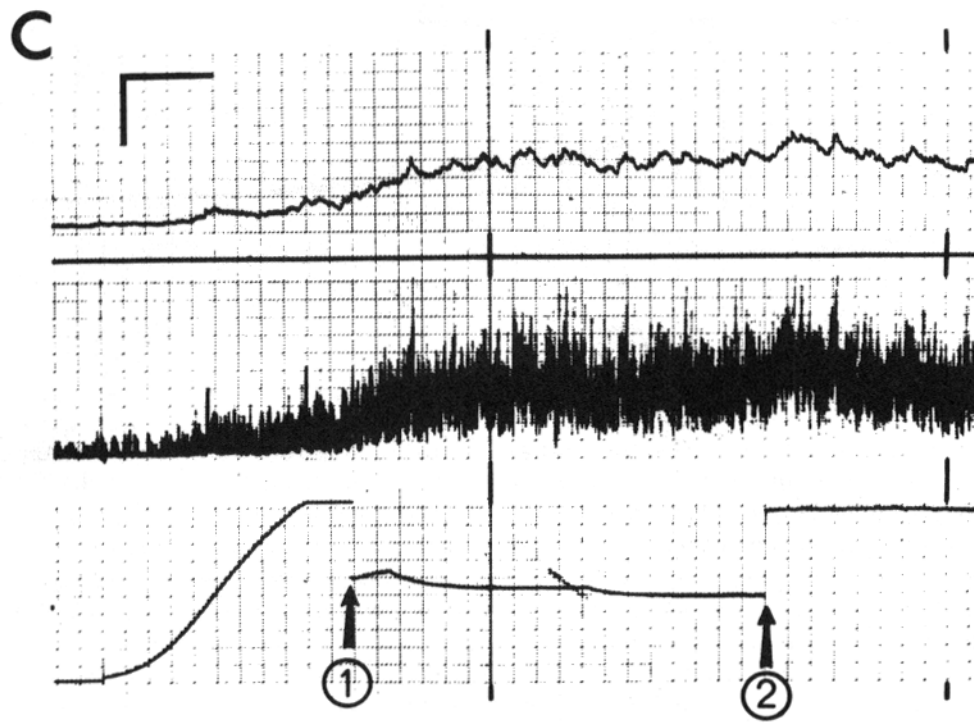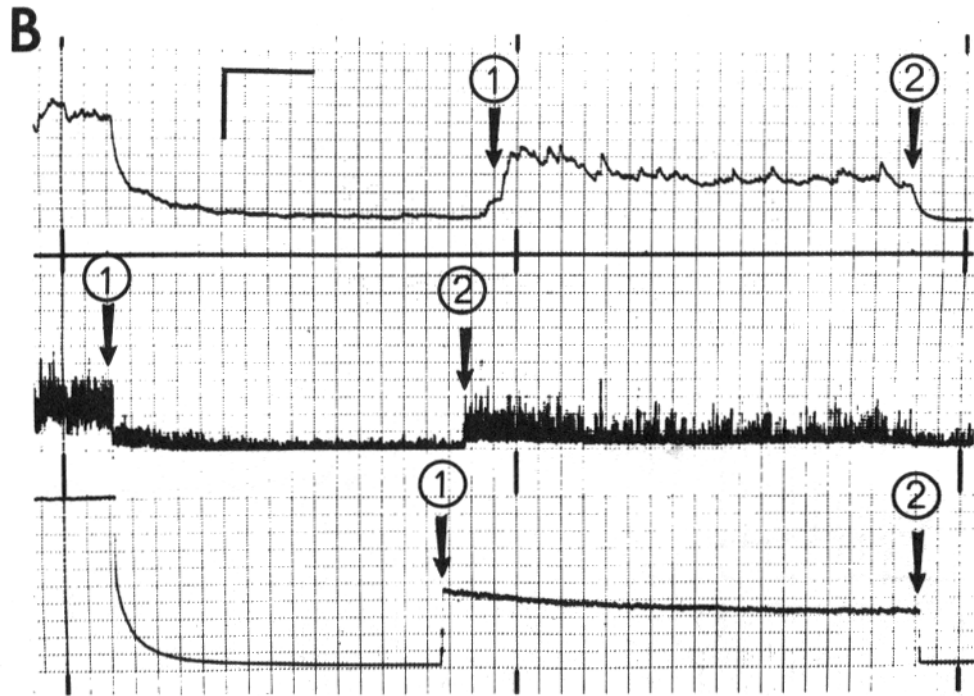
straight line, is reasonably well obeyed. The slope of the line is, however, shallower than we would expect from the voltage dependence for G_∞ in large bilayers. The slope of the line in Fig. 9 is such that n in Eq. 1 is 2.1, whereas n for large films is 5.2 (Muller et al., 1981). ($n = 1.0$ for the line of Fig. 7.) Although we cannot quantitatively account for this discrepancy, there are two known sources of bias in the comparison. First (as noted in the preceding paper), we certainly must miss counting channels that are so brief that we cannot distinguish them from the background noise. Given the exponential distribution of channel lifetimes, this is certain to make the log f_∞ vs. V
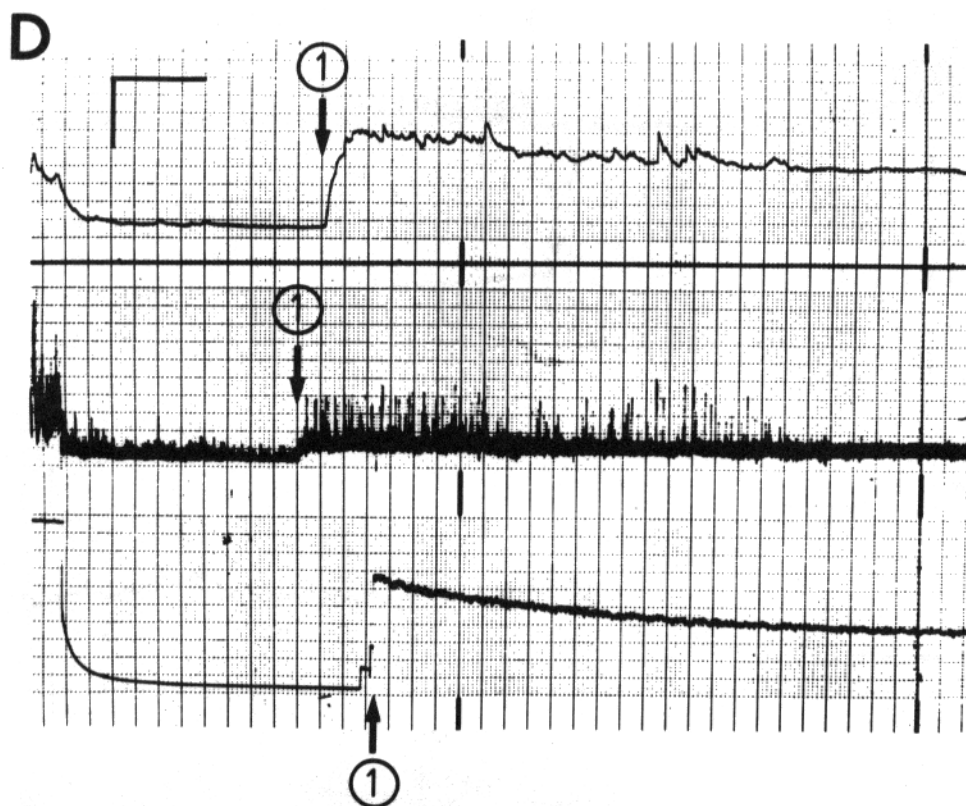

FIGURE 8.

characteristic appear to be too shallow. (This is the same source of error that caused our estimate of the average channel lifetime from the slope of the G_∞ vs. f_∞ line to be too great.) Second (as also discussed in the preceding paper), the strength of the voltage dependence of G_∞ is lower when G_∞ is measured at high V and low [Mon]. The value of $n = 5.2$ for large films is an average taken without regard to the voltage range in which n was measured. In fact, for the present experiment, we find that $n = 2.7$ when we measure it from the log G_∞-V line obtained from the low-pass-filtered record of the membrane current. In the Discussion, we will speculate on a possible basis for the reduced voltage dependence of G_∞ (or f_∞) at high V and low [Mon].

DISCUSSION

We believe that the work presented in this paper is sufficient to prove that the unitary conductance events characterized in the preceding paper are the same events that underlie the macroscopic monazomycin-induced conductance.
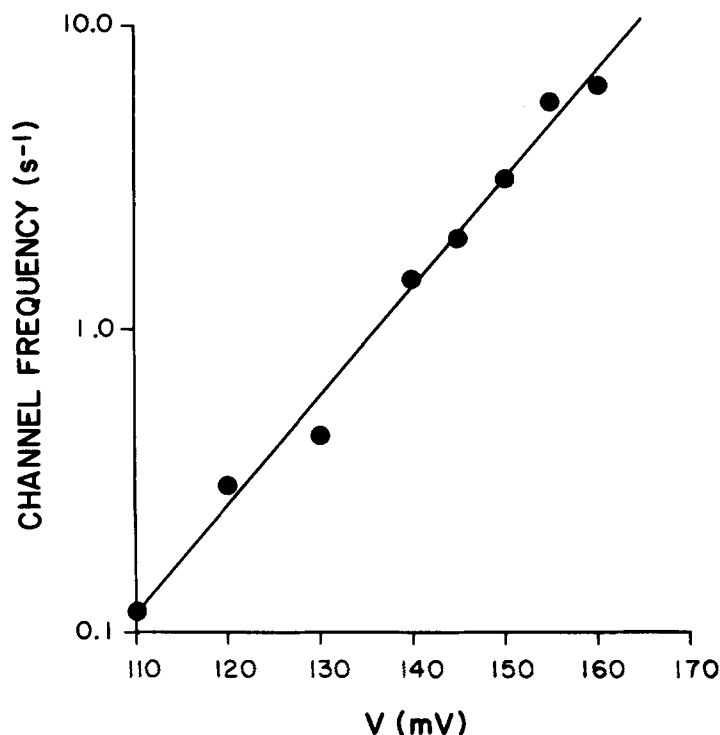

FIGURE 9. Log f_∞-V plot showing stronger voltage dependence than in Fig. 7. Here, the small film was taken from an already active large film. Each point represents the average of f_∞ at the applied V for two, three, or four 1-min runs. The f_∞ points were acquired with a descending series of voltage levels. The increased slope of the log f_∞-V line is not, however, caused by a downward drift of f at constant V. In the film whose behavior is illustrated in this figure, f was, if anything, actually increasing with time as can be shown by comparing the percentage change of f_∞ between the last two runs at each V; a positive change means that f_∞ has increased from the penultimate to the final run. For $V = 120$, 130, 140, 145, 150, 155, and 160 mV, the corresponding percentage changes of f_∞ are: 0.0, 0.0, 3.1, 2.6, 3.7, 14.0, and 16.9%. Thus, the trend of f with time is in the direction to weaken rather than strengthen the voltage dependence of f_∞.

The major arguments supporting this conclusion are:

(*a*) The conductances of a large and of a small bilayer vary in parallel when voltage steps are applied (Fig. 8) if the experiment is done with the correct protocol. In particular, this means avoiding the "kinetic trap" by taking the small film from a large one that is already active.

(*b*) This parallelism extends down to the level where we can resolve individual conductance jumps; the time-averaged conductance of the small

film shows S-shaped conductance increases and uninflected conductance decreases even at low levels of f (Fig. 8).

(c) When we can resolve the unitary events we find that f_∞ is directly proportional to G_∞ of the small film and that f_∞ is, as required, an exponential function of V (Fig. 9).

(d) Although we have not systematically investigated the dependence of f_∞ on [Mon], we find that a given level of f_∞ is associated with a less positive range of V if [Mon] is higher.

There are, in addition, two other arguments that are less obvious but are just as important. First, there is the demonstrated existence (Figs. 2-4) of a nonautocatalytic entry route for monazomycin operating in parallel with the autocatalytic pathway that is crucial in explaining the behavior of the macroscopic conductance (Muller and Peskin, 1981). (The inverse process, nonautocatalytic removal, is manifested as the sudden cessation of channel activity we often observe [Fig. 8D].) The presence of this nonautocatalytic route and the very low rate constants for the insertion and removal of monazomycin from the membrane are required (as argued in the theory section) if the autocatalytic model is to be non-self-contradictory. Second, the instantaneous kinetics of conductance changes are determined by (in the autocatalytic model) the surface concentration of a nonconducting oligomer (here designated $\widetilde{M}_3$). This implies that the local membrane characteristics near an $\widetilde{M}_3$ are in some sense different from the characteristics of unmodified membrane, far from any $\widetilde{M}_3$. Consequently, the membrane should become detectably inhomogeneous with respect to monazomycin channel activity at low [$\widetilde{M}_3$]. This inhomogeneity is an experimental fact, as shown in Figs. 5 and 6.

On the basis of the arguments listed above, we regard the connection between the macroscopic conductance and the unitary conductance events as established. The remainder of the Discussion will therefore focus mainly on some presently poorly understood features of this system and on possible ways to gain further information.

To begin, there is the issue of the weakened voltage dependence of G_∞ and f_∞ at low [Mon] and high V. This is unlikely to be caused by the transmembrane monazomycin flux, which is responsible for the phenomenon known as depletion inactivation (Heyer et al., 1976); we excluded depletion inactivation because we saw no sign of inactivation in large membranes when we simultaneously recorded the currents through large and small membranes under the conditions used to measure f_∞ (V). In addition, log G_∞-V characteristics obtained when significant depletion of the cis interfacial monazomycin is occurring are curvilinear (bending towards the V axis) (Heyer et al., 1976), whereas such characteristics are found to be linear in the present case (Fig. 9). Thus, the weakened dependence of G_∞ on V probably reflects a decreased voltage dependence of the serial reactions which lead to channel formation (reactions 6 and 7). One way in which this might occur is that the magnitude of the aggregation equilibrium constant (K_2 in reaction 7) could depend on membrane thickness, which is itself a function of V (Alvarez and Latorre, 1977).

An interesting alternative involves consideration of a second poorly understood property of the system, namely, the molecular basis for the voltage-dependent shift in the probability of the two conducting states of the monazomycin channels (Andersen and Muller, 1982). The most attractive interpretation of the shift is that it represents two different aggregation states of the channel such that an aggregate of lower molecularity becomes stabilized at high V.

Following Baumann and Mueller (1974) and Hanke and Boheim (1980), we may imagine that the two states are both barrels, which differ in diameter due to the addition (or removal) of one stave. If we further assume that the unitary conductance is proportional to the cross-sectional area of the lumen, one can calculate the ratio of the areas of peak-4 and peak-5 channels. If the channel cross section is a circle, and each monomer contributes a constant length to the circumference (independent of molecularity) we find

$$\frac{g_5}{g_4} = \frac{(S + 1)^2}{S^2} = 1 + \frac{2}{S} + \frac{1}{S^2}. \tag{9}$$

Given that $\frac{g_5}{g_4} = 1.37$, we find that $S = 5.86$, or rounding to the nearest molecule, $S = 6$. This is astonishingly close to the best estimate of the molecularity of the monazomycin channel from the dependence of G_∞ on [Mon] (Muller et al., 1981). Part of the reduced voltage dependence may thus directly reflect the reduced molecularity of the channel (see Muller and Peskin, 1981). Of course, this is all quite tenuous. Certainly, there are many reasons to believe that factors in addition to (or instead of) cross-sectional area will determine the unitary conductance (see, for instance, Finkelstein, 1975). For example, it is plausible that the position of one or more of the monomers making up the channel wall can vary (with V) in such a way that the ion-solvating properties of the wall decreases at high V.

We now turn briefly to the question of the physical basis of the autocatalytic and mass-action insertion reactions (reactions 6 and 8, respectively). That the rate constants for reaction 8 are very low is not particularly surprising, because the insertion of a monazomycin molecule presumably involves moving a charged amino group through the low dielectric constant membrane interior. If the entering species for reaction 8 is actually a trimer, the rate constants at $V = 0$ would likely be very low indeed. Thus, the real question is the nature of the mechanism by which the channel precursors $(\tilde{M}_3)$ lower the energy barrier for insertion of more M_3. At present, our best guess is that the potential lumen of the $\tilde{M}_3$, which is envisaged to be a polar region, provides a low activation-energy tunnel through the oily part of the membrane. Alternatively, it is possible that an $\tilde{M}_3$ disrupts the bilayer structure so that an M_3 can slip alongside an existing $\tilde{M}_3$.

Finally, we would like to emphasize the need for a stochastic model that contains the following features: (*a*) in the limit of high channel activity, it should reduce to the continuous autocatalytic scheme; (*b*) the model should incorporate the existence of the required nonautocatalytic entry and exit processes; (*c*) the model should explicitly make provision for lateral diffusion

of monazomycin in the plane of the membrane. Two uses for such a model come quickly to mind. The first is a description of how the monazomycin in the membrane is distributed during changes of G. As we mentioned in the Results, we anticipate that a radially symmetrical wave of monazomycin activity will spread out from the entry point of a pioneer molecule during increases of G. Second, such a model would allow numerical calculations of fluctuations at any desired value of G. This will in turn permit us to test if the properties (individual or ensemble) of channels change as the surface concentration of monazomycin goes to values higher than those which permit unitary conductance jumps to be resolved. In particular, it would be very nice if the noise measurements done by Kolb (1979) could be reproduced just by turning the crank of the proposed model. In closing, we should state that we realize that the properties of the desired model are so complex as to require a "brute force" approach in which the location and state of each molecule is calculated separately.

REFERENCES

ALVAREZ, O., and R. LATORRE. 1978. Voltage-dependent capacitance in lipid bilayers made from monolayers. *Biophys. J.* **21:**1–17.

ANDERSEN, O. S., and R. U. MULLER. 1982. Monazomycin-induced single channels. I. Characterization of the elementary conductance events. *J. Gen. Physiol.* **80:**403–426.

BAMBERG, E., and K. JANKO. 1976. Single channel conductance at lipid bilayer membranes in presence of monazomycin. *Biochim. Biophys. Acta.* **426:**447–450.

BAUMANN, G., and P. MUELLER. 1974. A molecular model of membrane excitability. *J. Supramol. Struct.* **2:**538–557.

FINKELSTEIN, A. 1975. Discussion paper. *Ann. N. Y. Acad. Sci.* **264:**244–246.

HANKE, W., and G. BOHEIM. 1980. The lowest conductance state of the alamethicin pore. *Biochim. Biophys. Acta.* **596:**456–462.

HEYER, E. J., R. U. MULLER, and A. FINKELSTEIN. 1976. Inactivation of monazomycin-induced voltage-dependent conductance in thin lipid membranes. II. Inactivation produced by monazomycin transport through the membrane. *J. Gen. Physiol.* **67:**731–748.

KOLB, H.-A. 1979. Conductance noise of monazomycin-doped bilayer membranes. *J. Membr. Biol.* **45:**277–292.

MULLER, R. U., and O. S. ANDERSEN. 1975. Single monazomycin channels. 5th International Biophysics Congress. U. Lassen and J. O. Wieth, editors. *Abstract 367.*

MULLER, R. U., and O. S. ANDERSEN 1981. Initiation of monazomycin single-channel activity. *Biophys J.* **33:**64a.

MULLER, R. U., and A. FINKELSTEIN. 1972. Voltage-dependent conductance induced in thin lipid membranes by monazomycin. *J. Gen. Physiol.* **60:**263–284.

MULLER, R. U., G. ORIN, and C. S. PESKIN. 1981. The kinetics of monazomycin-induced voltage-dependent conductance. I. Proof of the validity of an emperical rate equation. *J. Gen. Physiol.* **78:**171–200.

Muller, R. U., and C. S. Peskin. 1981. The kinetics of monazomycin-induced voltage-dependent conductance. II. Theory and a demonstration of a form of memory. *J. Gen. Physiol.* **78**:201–229.

Nakayama, H., K. Furihata, H. Seto, and N. Ōtake. 1981. Structure of monazomycin, a new ionophorous antibiotic. *Tetrahedron Lett,* **22**:5217–5220.